BEAM DYNAMICS STUDIES FOR THE SPS-II 3-GeV BOOSTER SYNCHROTRON WITH 270-MeV LINAC INJECTOR*

S. Jummunt†, T. Yan, P. Boonpornprasert, S. Chunjarean, P. Sunwong, P. Sudmuang, P. Klysubun
Synchrotron Light Research Institute, Nakhon Ratchasima, Thailand

Abstract

The Siam Photon Source II (SPS-II) booster synchrotron plays a crucial role in delivering high-quality electron beams, enabling efficient injection, and ensuring stable and reliable operation of the fourth-generation storage ring. To improve booster performance and operational robustness, the linear accelerator (linac) injection energy has been upgraded to 270 MeV. This work presents comprehensive beam dynamics studies of the SPS-II booster during energy ramping from 270 MeV to 3 GeV. Particle-tracking simulations were performed under realistic operating conditions, including synchrotron radiation effects, multipole field errors, residual closed-orbit distortions, and aperture constraints. The simulation results demonstrate stable beam acceleration and high transmission efficiency throughout the energy ramping cycle.

INTRODUCTION

The Siam Photon Source II (SPS-II) storage ring is based on a double triple-bend achromat (DTBA) lattice designed to achieve a natural emittance below 1 nm·rad while supporting a stored beam current of 300 mA [1]. As the SPS-II design has progressed, several machine parameters have been refined through accelerator physics studies, including an updated RF frequency of 499.654 MHz [2] and an increase in the linac injection energy to 270 MeV.

The SPS-II booster is designed to accelerate the injected beam from the linac to 3 GeV while preserving beam quality for efficient storage-ring injection. To reduce construction costs, the booster adopts a concentric design with a minimized number of magnets and power-supply families. A FODO lattice with combined-function magnets is selected to achieve a low beam emittance of 5.89 nm·rad. In addition, the booster operates at a repetition rate of 2 Hz to support efficient top-up injection and short filling time [3]. The booster lattice and operating conditions have been systematically optimized through beam dynamics simulations under realistic machine conditions, including magnetic field errors, multipole components, magnet misalignments, residual orbit distortions, and aperture limitations [4].

The studies indicate that beam injection and the early stage of energy ramping are the most critical operating conditions affecting beam capture and transmission efficiency. Therefore, this work focuses on the investigation of injection efficiency and beam dynamics performance during energy ramping with 270 MeV injection.

* Work supported by Synchrotron Light Research Institute, Thailand
† siriwan@slri.or.th

UPGRADE OF LINAC INJECTION ENERGY

The original SPS-II injector design was based on a 150-MeV linac. At this low injection energy, the dipole magnets operate at low excitation current, where magnetic field stability and reproducibility become less reliable. Consequently, the injection process becomes highly sensitive to magnetic imperfections and beam mismatch, leading to orbit distortion, reduced beam capture efficiency, and beam loss during the early stage of energy ramping.

To improve injection efficiency and operational robustness, two approaches were investigated: enlarging the vacuum chamber aperture and increasing the linac injection energy [5]. Although a larger aperture could relax acceptance constraints, it would require larger magnet bores and more complex magnet and power-supply designs. Therefore, increasing the injection energy to 270 MeV was identified as the more practical and effective solution.

The higher injection energy improves magnetic field reproducibility through increased dipole operating current. Together with the enhanced beam quality provided by the upgraded linac, these improvements lead to better injection matching, higher beam capture efficiency, and more robust booster operation. However, only a single bunch with a maximum charge of 0.42 nC is generated by the linac and accelerated through the booster. Therefore, to minimize the injection time and ensure efficient storage-ring filling, the booster design emphasizes low-loss injection, stable energy ramping, and high transmission efficiency during acceleration from 270 MeV to 3 GeV.

SIMULATION MODEL AND MACHINE CONDITIONS

To evaluate booster performance under realistic operating conditions, beam dynamics simulations include magnetic field errors, multipole field components, magnet misalignments, residual closed-orbit distortions, and physical aperture constraints. The simulations were performed using the ELEGANT code [6].

Injected Beam Parameters

The injected linac beam is assumed to have an energy of 270 MeV, with a geometric transverse emittance of 10 nm·rad in both transverse planes and an energy spread of 0.36%. The linac provides a single-bunch charge of 0.42 nC. The beam is transported through the low-energy beam transport (LBT) and matched at the end of the kicker magnet, which is defined as the booster injection point. Detailed linac beam parameters will be reported elsewhere.

Multipole Errors

Multipole errors are unwanted higher-order magnetic field components arising from magnet imperfections, manufacturing tolerances, and alignment errors. These errors can perturb beam motion and reduce the dynamic aperture. Acceptable multipole error levels of 2×10^{-4} for dipole magnets and 5×10^{-4} for quadrupole and sextupole magnets were used in the simulations.

Magnetic Errors and Residual Orbit Distortions

Magnet misalignments and magnetic field errors generate closed-orbit distortions that can be partially corrected using orbit correction and magnet tuning. The assumed alignment and field error tolerances are based on Ref. [7]. However, to evaluate realistic machine performance, simulations were performed including residual closed-orbit distortions of 2 mm and 1 mm for horizontal and vertical planes, respectively. Under these assumptions, magnetic field errors of 1%, transverse and longitudinal misalignments of 50 μm, and small roll-angle errors were applied.

Aperture Requirement and Beam Stay-Clear

The aperture requirements are defined by the beam stay-clear (BSC), which specifies the minimum acceptable vacuum chamber and magnet apertures. The BSC is evaluated from the transverse beam envelopes, taking into account the effects of beam emittance, energy spread, dispersion, residual orbit distortions, and beam oscillations [3]. The required aperture diameters are 32.68 mm for the QF quadrupole magnets and 18.30 mm for the dipole magnets. These values define the baseline aperture required for beam survival during injection and energy ramping, as further verified by multiparticle tracking simulations in the following section.

ENERGY RAMPING PERFORMANCE

The injected beam from the 270 MeV linac is matched to the booster optics. Particle tracking at injection shows a transverse acceptance of approximately ±4 mm at the kicker location with 100% beam transmission through the kicker magnet during injection. However, overall beam survival during acceleration also depends on beam quality, magnetic errors, and physical aperture limitations. Therefore, particle tracking simulations during energy ramping are required to evaluate booster performance under realistic operating conditions.

Ramping Pattern

The SPS-II booster operates at a repetition rate of 2 Hz with a sinusoidal ramp cycle, as shown in Figure 1. To maintain thermal stability of the magnet yoke during top-up operation, the dipole current is initially maintained at the equivalent 50 MeV level and then increased to the 270 MeV level over 53.30 ms before the main energy ramping cycle begins. The beam energy is then ramped from 270 MeV to 3 GeV within 0.25 s, followed by a 10 ms flat-top period for stable beam extraction. The cycle is completed by ramping the beam energy down over 196.7 ms, resulting in a total cycle duration of 500 ms.

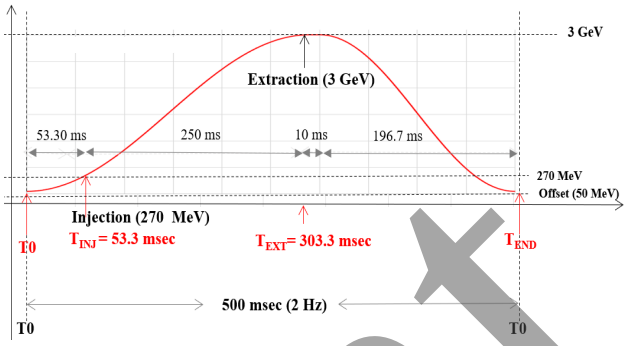

Figure 1: Booster ramping cycle with a repetition rate of 2 Hz.

Figure 2 shows the RF ramping profile generated using the *computeRfRamp* script from the ELEGANT booster-Ramp example. The script automatically calculates the RF parameters, providing a self-consistent RF voltage profile during acceleration from 270 MeV to 3 GeV over a 250 ms ramping cycle. The RF voltage is increased from 400 kV at injection to 1.0 MV during the first 150 ms of the ramp, followed by a constant voltage of 1.0 MV between 150 ms and 250 ms to maintain stable beam acceleration.

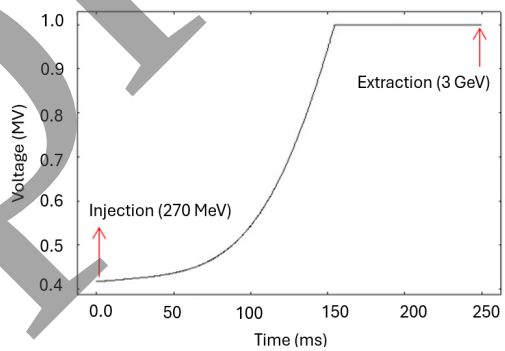

Figure 2: RF voltage ramping pattern during booster energy ramping.

Beam Dynamics During Energy Ramping

The energy ramping process plays a key role in beam stability and overall booster performance. To evaluate realistic machine performance, full-cycle particle tracking simulations were carried out including synchrotron radiation effects, magnetic field errors, multipole field errors, and residual closed-orbit distortions. A minimum transmission efficiency of 90% throughout the ramping cycle was adopted as the design target.

Simulation results show that the aperture estimated solely from the beam stay-clear analysis is insufficient to accommodate beam growth during energy ramping. Using the initial vacuum chamber diameters of 32.68 mm in the straight sections and 18.30 mm in the dipole sections, under these conditions, the ramping survival rate was found to be below 80 %, indicating that the aperture is the primary limiting factor.

After aperture optimization to ensure a beam survival rate of more than 90%, the vacuum chamber diameters were increased to 40 mm in the straight sections and 21 mm in the dipole sections. With this adjustment, the transmission efficiency improves to 98%, as shown in Figure 3. In addition, off-momentum tracking studies were performed with a relative momentum deviation of $\delta = 0.5\%$ to evaluate sensitivity to energy errors. Under this condition, the beam survival rate is reduced to 92%, still within the acceptable operating margin. These results confirm that the selected aperture configuration provides sufficient acceptance and robust performance under both on-momentum and off-momentum conditions.

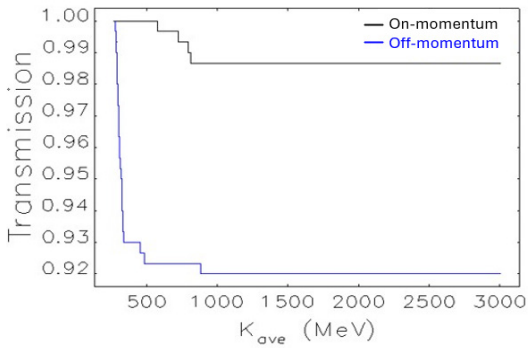

Figure 3: Beam survival during the booster energy ramping with all errors, aperture limit and residual orbit distortion.

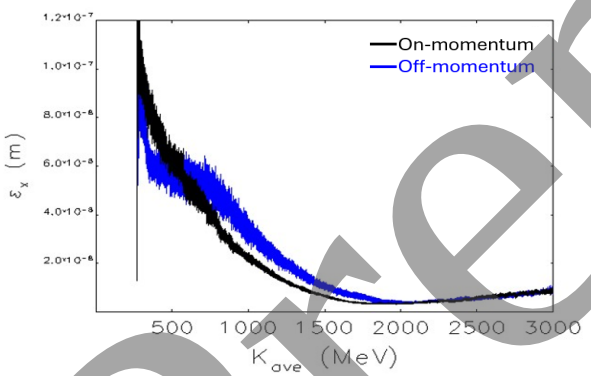

Figure 4: Evolution of horizontal emittance during the booster energy ramping.

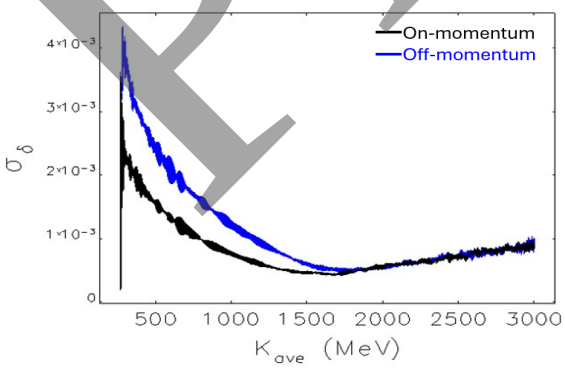

Figure 5: Evolution of energy spread during the booster energy ramping.

Figure 4 and Figure 5 present the evolution of horizontal emittance and energy spread during booster energy ramping, respectively. In the off-momentum case, the horizontal emittance reaches 8.04 nm·rad, with a corresponding energy spread of 8.55×10^{-4}. Although an increase in emittance is observed, the final value at 3 GeV remains below 10 nm·rad, thereby satisfying the acceptance criterion for efficient injection into the storage ring.

CONCLUSION

Beam dynamics studies of the SPS-II 3 GeV booster with 270 MeV linac injection were performed under realistic machine conditions. Particle-tracking simulations demonstrate stable beam acceleration from 270 MeV to 3 GeV with sufficient operational margin. Increasing the injection energy to 270 MeV improves beam capture efficiency, reduces sensitivity to magnetic imperfections, and enhances beam survival during energy ramping. The studies also show that the aperture estimated solely from beam stay-clear analysis is insufficient under realistic error conditions. By increasing the vacuum chamber aperture to 40 mm in the straight sections and 21 mm in the dipole sections, a beam transmission efficiency greater than 90% is achieved throughout the energy ramping cycle.

Further optimization of the ramping pattern and injection configuration is ongoing to reduce beam loss, improve beam acceptance, and enhance operational robustness.

ACKNOWLEDGEMENTS

The authors would like to express their sincere gratitude to the international advisors from RIKEN and NSRRC for their valuable guidance, contributions, and continued support in the booster design and simulation studies.

REFERENCES

[1] P. Klysubun, T. Pulampong, and P. Sudmuang, "Design and optimisation of SPS-II storage ring", in *Proc. IPAC'17*, Copenhagen, Denmark, May 2017, pp. 2773-2775. doi:10.18429/JACoW-IPAC2017-WEPAB086

[2] P. Sudmuang *et al.*, "SPS-II project: Status update", *in Proc. IPAC'25*, Taipei, Taiwan, May. 2025, pp. 903-908. doi:10.18429/JACoW-IPAC2025-TUZD2

[3] S. Krainara, S. Klinkhieo, P. Klysubun, T. Pulampong, and P. Sudmuang, "Conceptual design of booster synchrotron for Siam Photon Source II", in *Proc. IPAC'21*, Campinas, Brazil, May 2021, pp. 2795-2797. doi:10.18429/JACoW-IPAC2021-WEPAB089

[4] S. Jummunt, S. Klinkhieo, P. Klysubun, T. Pulampong, and P. Sudmuang, "Energy ramping process for SPS-II booster", in *Proc. IPAC'22*, Bangkok, Thailand, Jun. 2022, pp. 527-530. doi:10.18429/JACoW-IPAC2022-MOPOTK034

[5] S. Jummunt, P. Sunwong, P. Sudmuang, T. Phimsen, and P. Klysubun. "Design progress of the booster synchrotron for Siam Photon Source II", in *Proc. IPAC'25*, Taipei, Taiwan, May. 2025, pp. 2047-2050. doi:10.18429/JACoW-IPAC2025-WEPM037

[6] M. Borland, "ELEGANT: A flexible SDDS-compliant code for accelerator simulation", Argonne National Laboratory, Lemont, IL, USA, Rep. LS-287, 2000. doi:10.2172/761286

[7] NSRRC, private communication.